

Overview experimental validation data for zoned model of hepatic glucose metabolism

Periportal & perivenous hepatocytes (Cell Scale)

Incorporation of lactate and glucose in glycogen periportal and perivenous (Peak1990 [1])

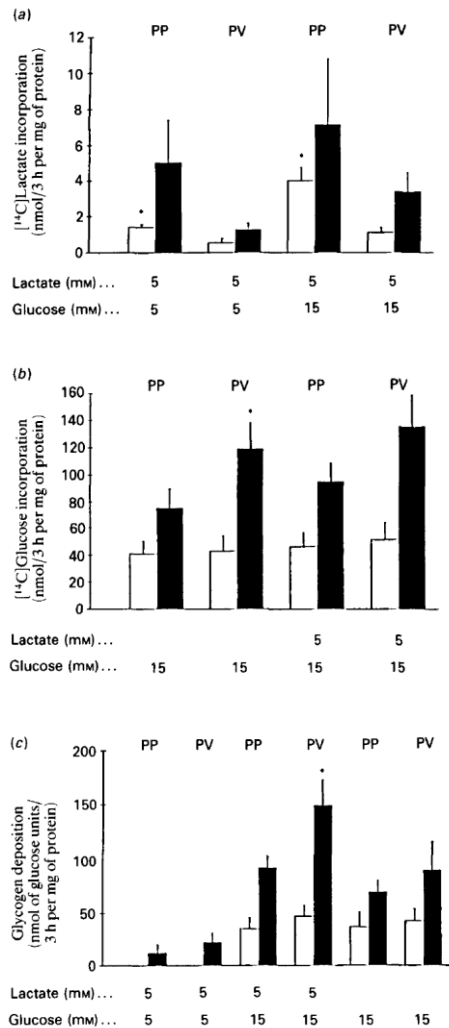


Fig. 1. Incorporation of (a) $[^{14}\text{C}]$ lactate and (b) $[^{14}\text{C}]$ glucose into glycogen and (c) glycogen deposition in periportal and perivenous hepatocytes

Lactate formation and glucose production depending on glucose and lactate (Probst1982 [2])

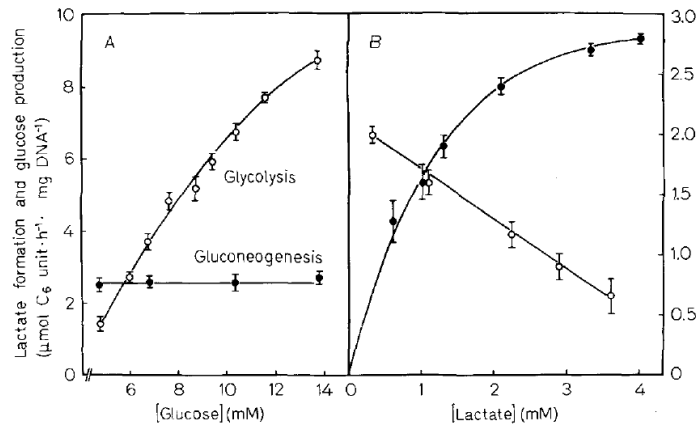


Fig. 1. Rate of glycolysis and gluconeogenesis as a function of glucose and lactate concentration. Cells were cultured on floating collagen gels for 48 h under basic conditions with 0.5 nM insulin and 0.1 μM dexamethasone. Using these basic hormone concentrations, metabolic rates were determined radiochemically by incubating the cells for another 2 h with radioactive substrates. Glycolysis was measured using [^{14}C]-glucose in the presence of unlabelled lactate. Gluconeogenesis was assayed using [^{14}C]lactate in the presence of unlabelled glucose. (A) The concentration of glucose was varied, that of lactate was kept constant at 2 mM; (B) the concentration of glucose was kept constant at 5 mM and that of lactate was varied. Values are means \pm SEM of six culture dishes from two different cell preparations

Short-term effect of insulin on gluconeogenesis & glycolysis (Probst1982 [2])

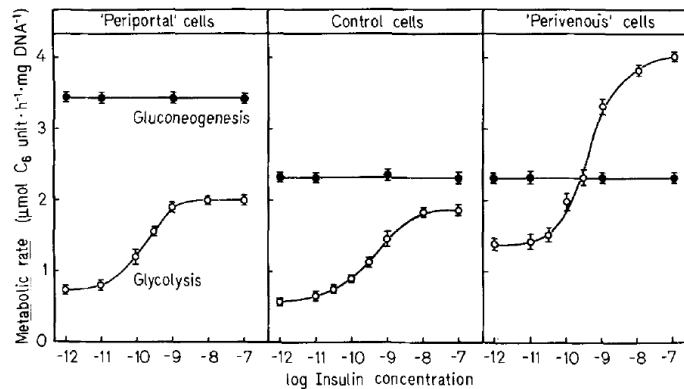


Fig. 3. Short-term effect of insulin concentration on glycolytic and gluconeogenic rates in cultured hepatocytes resembling periportal and perivenous cells. 'Perivenous' hepatocytes were cultured on plastic dishes with insulin, 'periportal' cells with glucagon as the dominant hormone and control cells under basic conditions as described in Fig. 2. After 46 h they were incubated in insulin and glucagon-free media two times for 2 h. Medium was changed again, then containing the initial concentrations of insulin as indicated (log M). Cells were incubated with ^{14}C -labelled substrates for 1.5–2 h. Values represent means \pm SEM of three culture dishes from one typical experiment out of three

Short-term effect of glucagon concentration (Probst1982 [2])

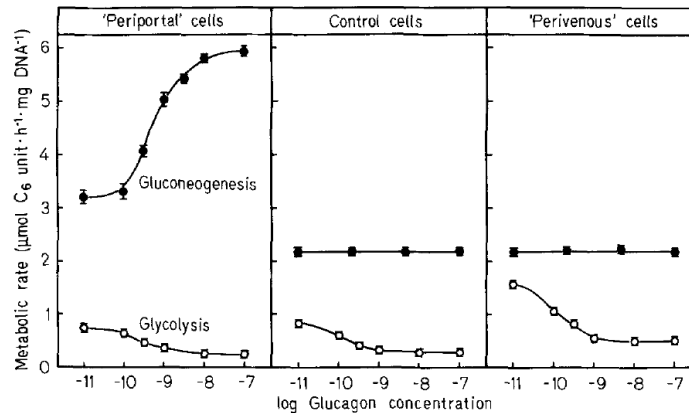


Fig. 4. Short-term effect of glucagon concentration on glycolytic and gluconeogenic rates in cultured hepatocytes resembling periportal and perivenous cells. 'Perivenous' cells were cultured on plastic dishes with insulin, 'periportal' cells with glucagon as the dominant hormone and control cells under basic conditions as described in Fig. 2. For the study of glycolysis cells were washed as described in Fig. 3. For the assay of gluconeogenesis, cells were washed twice rapidly within 5 min with medium containing the initial glucagon concentrations shown (log M). Cells were incubated with ^{14}C -labelled substrates for 1 h (gluconeogenesis) or 2 h (glycolysis). Values represent means \pm SEM of three culture dishes from one typical experiment out of three

Relationship between rates of glucose production and lactate concentration (and effect epinephrine) (Matsumura1984 [3])

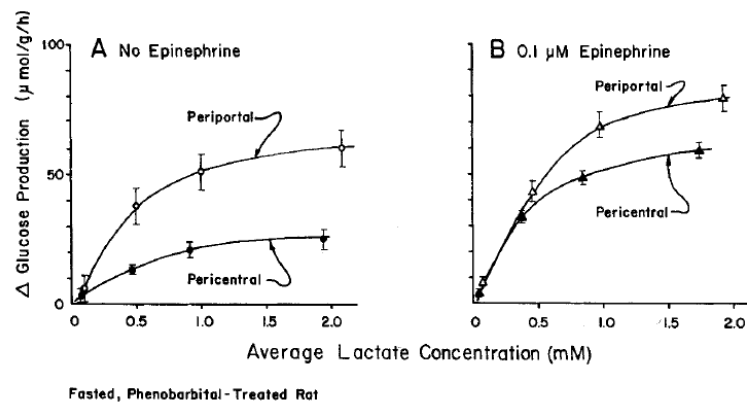


Fig. 3. Relationship between rates of glucose production and lactate concentration in periportal and pericentral regions of the liver lobule. Rates of oxygen uptake were measured in periportal and pericentral regions of the liver lobule in the presence and absence of lactate as shown in Fig. 2. Rates of glucose production were calculated from the extra O_2 taken up locally. Abscissa: average lactate concentrations in periportal and pericentral regions were calculated as follows: [inflow] - ([inflow] - [outflow])/4 and [outflow] + ([inflow] - [outflow])/4, respectively. This equation estimates the lactate concentration 1/4 and 3/4 of the way through the liver lobule. Ordinate: increases in rates of glucose production in periportal (\circ , Δ) and pericentral areas (\bullet , \blacktriangle) due to the addition of lactate in the presence (Δ , \blacktriangle) and absence (\circ , \bullet) of 0.1 μM epinephrine. (A) No epinephrine; (B) 0.1 μM epinephrine. Mean \pm SEM, $n = 5$

Dependence of net glucose flux on glucose-6-phosphate (Jungermann1982 [4, 5])

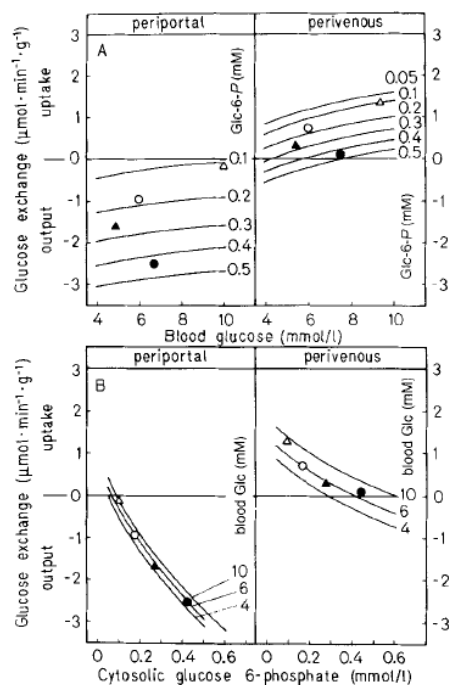


Fig. 3. Dependence of the net flux of glucose in the periportal and perivenous zone of rat liver parenchyma on the concentrations of blood glucose (A) and of cytosolic glucose 6-phosphate (B). Glc, glucose; Glc-6-P, glucose 6-phosphate. The principle of the calculation, the enzyme activities (V) and affinities (K_m) have been described under Materials and Methods. The range of physiological substrate concentrations considered for glucose was 4–10 mM (Table 3). The lower value may be reached after 48 h starvation [50], the higher one after a meal [51] (Balks, Katz and Jungermann, unpublished). The range considered for glucose 6-phosphate was 0.1–0.5 mM (Table 3). Net flux is given by the difference between the flux of the glucokinase and of the glucose-6-phosphatase reaction. Specific physiological conditions: (○) fed; (●) fed, glucagon-treated; (Δ) eating; (▲) fasting

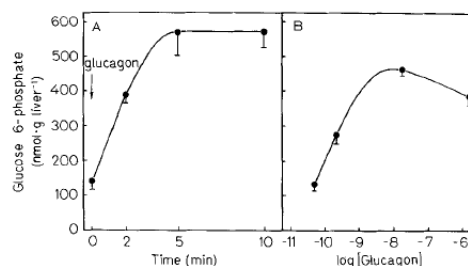


Fig. 2. Increase by glucagon of the level of glucose 6-phosphate in the liver of fed rats. (A) Time course at a glucagon concentration of 1.5 μmol/l. (B) Dependence on the glucagon concentration 2 min after injection of the hormone. Glucagon was injected after 45 min of narcosis, and the concentration expressed in mol·l⁻¹. Liver tissue was fixed thereafter at the time intervals indicated. Each point represents the mean ± standard deviation (S.D.) of three animals

Time course effects of glucagon on glucose output (Shiota1995 [6])

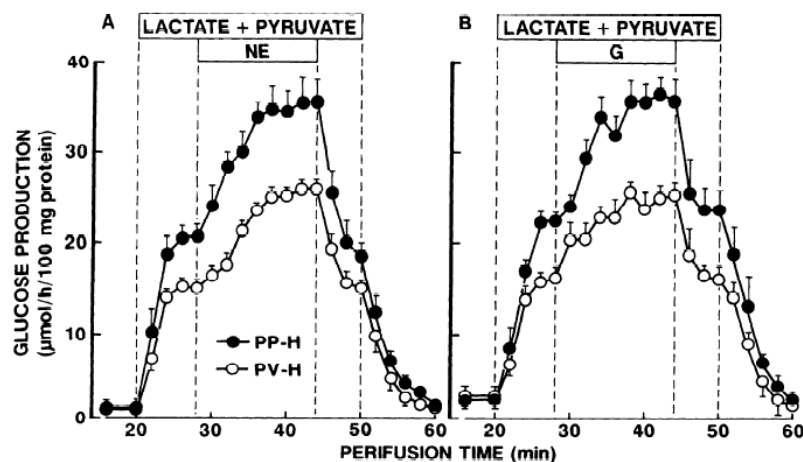


Fig. 1. Time course of effects of norepinephrine (NE) and glucagon (G) on gluconeogenesis in perfused periportal (PP-H) and perivenous (PP-V) hepatocytes. Cells were isolated from rats starved for 24 h. PP-H and PP-V were first perfused with medium that contained no substrates at a flow rate of 3 ml/min for 20 min, and then perfusion was continued with 10 mM lactate + 1 mM pyruvate. Substrates, 100 nM NE and 100 nM glucagon, were infused for times indicated. Data are means ± SE of results from 8 experiments.

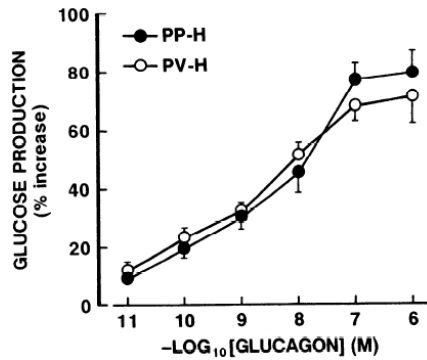


Fig. 3. Effects of increasing concentrations of glucagon on gluconeogenesis in perfused PP-H and PV-H. Cells were isolated from control rats starved for 24 h and were perfused as described in legend to Fig. 1. Rates of glucose production established after perfusion for 16 min with glucagon are expressed as percentage change from rate with substrates alone. Data are means \pm SE of results from 4–10 experiments.

Dose response of gluconeogenesis in periportal and perivenous hepatocytes (Tosh1988 [7])

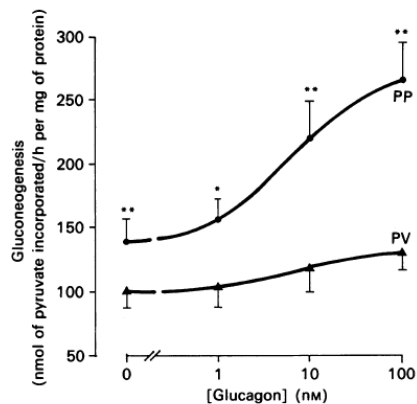


Fig. 1. Dose-response curve to glucagon of gluconeogenesis in periportal and perivenous hepatocytes

Hepatocytes isolated from the periportal or perivenous zones of rat liver were cultured with the concentrations of glucagon shown for 14 h. Gluconeogenesis was determined during a subsequent 2 h incubation in hormone-free medium containing 0.6 mM-[3- 14 C]-pyruvate, 0.75 mM-palmitate and 0.5 mM-L-carnitine. Rates of gluconeogenesis are expressed as nmol of pyruvate incorporated into glucose/h per mg of cell protein. Values are means and s.e.m. bars for 14 periportal (PP, ●) and 14 perivenous (PV, ▲) preparations. Significant differences between periportal and perivenous values are shown by: * $P < 0.01$; ** $P < 0.005$.

Effect of glucagon on glucose output (Ikezawa1998 [8])

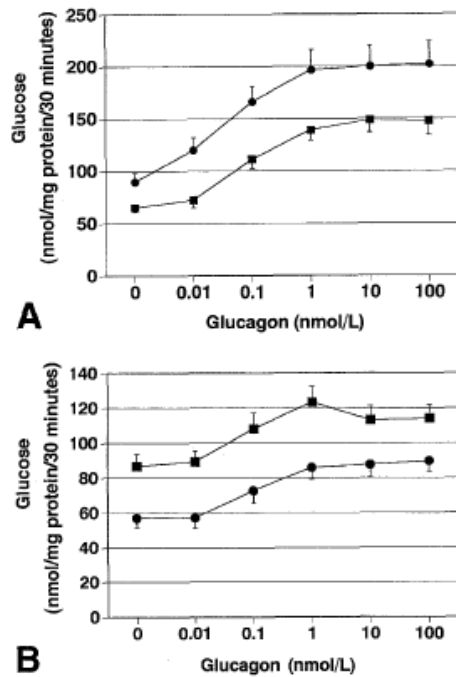


Fig 1. The effect of glucagon on glucose output from PPHs (■, n = 6) and PVHs (●, n = 6) of fed normal Wistar rats (A) and on glucose output with gluconeogenic substrates (5 mmol/L lactate, 0.5 mmol/L pyruvate, and 5 mmol/L L-alanine) from PPHs (■, n = 6) and PVHs (●, n = 6) of 24-hour fasted normal Wistar rats (B). The glucose outputs without glucagon or gluconeogenic substrates were 17.2 ± 3.7 nmol/mg protein/30 minutes in PPHs and 12.4 ± 1.4 nmol/mg protein/30 minutes in PVHs.

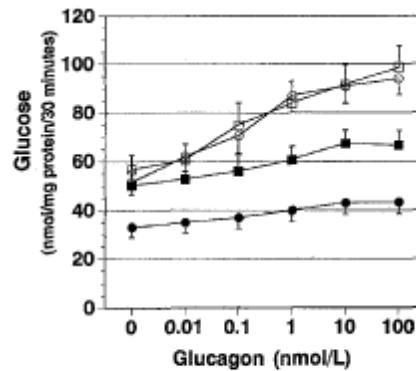


Fig 5. The effect of glucagon on glucose output with gluconeogenic substrates (5 mmol/L lactate, 0.5 mmol/L pyruvate, and 5 mmol/L L-alanine) from PPHs (□, n = 6) and PVHs (○, n = 6) of 24-hour fasted diabetic or PPHs (■, n = 6) and PVHs (●, n = 6) of nondiabetic BB rats.

Effect of insulin on glycogen and lactate output (Ikezawa2001 [8])

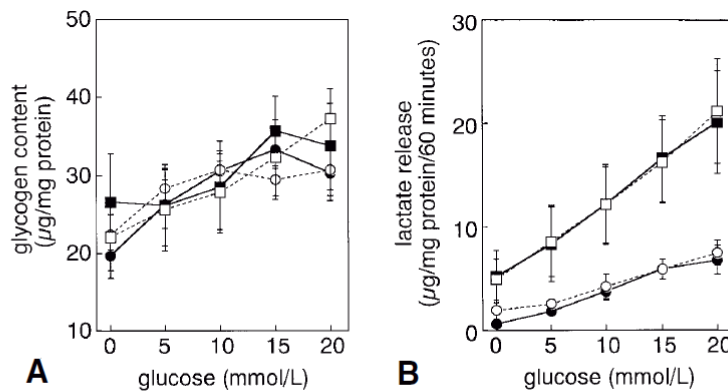


Fig 1. Effects of insulin on glycogen synthesis (A) and glycolysis (B) in PPHs and PVHs. PPHs (circles) and PVHs (squares) isolated from fed rats were incubated with glucose alone (filled symbols) or glucose with 10 nmol/L insulin (open symbols) for 1 hour. Each point shows the mean \pm SE (n = 6).

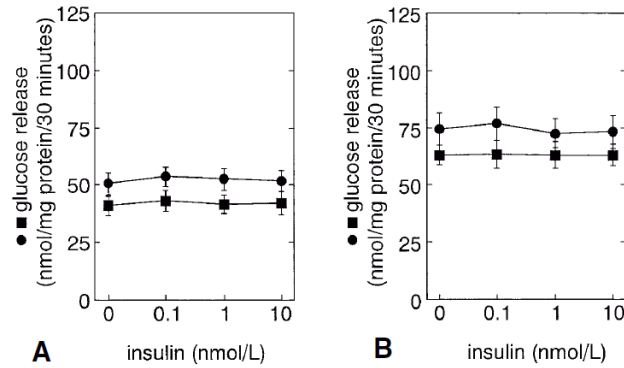


Fig 2. Effect of insulin on gluconeogenesis in PPHs and PVHs. PPHs (circles) and PVHs (squares) isolated from 24-hour fasted rats were incubated with gluconeogenic substrates (5 mmol/L lactate, 0.5 mmol/L pyruvate, and 5 mmol/L L-alanine) and insulin (A) or gluconeogenic substrates, 0.2 nmol/L glucagon, and insulin (B) for 30 minutes. Symbols, Glucose released into medium. Each point shows the mean \pm SE (n = 6).

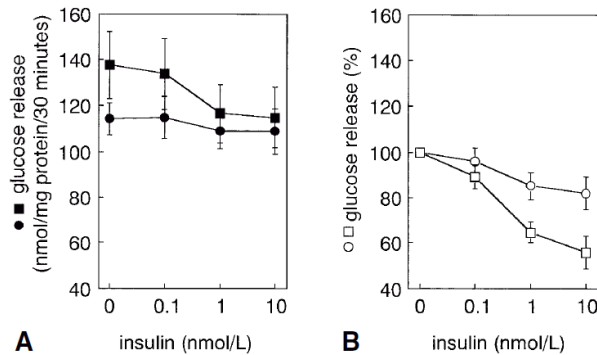


Fig 3. Effect of insulin on glucagon-induced glycogenolysis in PPHs and PVHs. PPHs (circles) and PVHs (squares) isolated from fed rats were incubated with 0.1 nmol/L glucagon with insulin for 30 minutes. Filled symbols, Glucose released into the medium (A); open symbols, relative antagonizing effect of insulin on 0.1 nmol/L glucagon-induced glucose release (B). Each point shows the mean \pm SE (n = 12).

Relative fluxes periportal and perivenous (Jones1996 [9])

Metabolic Fluxes, J_{GLUCOSE} , J_{PK} , and J_{PEPCK} in Hepatocytes Isolated from the Periportal and the Perivenous Zones

	Periportal (nmol/mg wet wt/15 min)	Perivenous	PP/PV
J_{GLUCOSE}	18.4 ± 1.8	$13.0 \pm 1.4^*$	1.42 ± 0.06
J_{PK}	3.3 ± 0.3	3.1 ± 0.6	1.06 ± 0.08
J_{PEPCK}	21.7 ± 1.8	$16.8 \pm 0.7^*$	1.29 ± 0.09
$J_{\text{GLUCOSE}}/J_{\text{PEPCK}}$ (%)	84 ± 2	$77 \pm 3^*$	1.09 ± 0.02
$J_{\text{PK}}/J_{\text{PEPCK}}$ (%)	16 ± 2	$23 \pm 3^*$	0.69 ± 0.1

Note. Hepatocytes (6 mg/ml) were incubated in the presence of 1.0 mM lactate plus 0.1 mM pyruvate and $\text{NaH}^{14}\text{CO}_3$ ($0.15 \mu\text{Ci}/\mu\text{mol}$) for 15 min. Incorporation of $^{14}\text{CO}_2$ into glucose, lactate, and pyruvate was measured as described under Materials and Methods. Results are expressed as means \pm SEM for five cell preparations. Statistical analysis was by two-way analysis of variance.

* Statistical differences between periportal and perivenous cells, $P < 0.05$.

Zonation of [1-¹⁴C]Lactate plus Pyruvate Metabolism in Periportal and Perivenous Hepatocytes

Control	Periportal (nmol/mg wet wt/15 min)	Perivenous	PP/PV
Incorporation of [1- ¹⁴ C]lactate + pyruvate into glucose	9.0 ± 1.2	3.9 ± 0.5*	2.31 ± 0.10
Oxidation of [1- ¹⁴ C]lactate + pyruvate	14.8 ± 2.4	11.4 ± 2.6*	1.30 ± 0.08
Oxidation of [2- ¹⁴ C]lactate + pyruvate	2.1 ± 0.7	2.4 ± 0.8	0.88 ± 0.04
<i>F'</i> factor	1.19 ± 0.03	1.31 ± 0.06*	0.91 ± 0.01
$J_{ME} + J_{PEPCK}$	10.7 ± 1.3	5.6 ± 0.9*	1.91 ± 0.03
J_{PC}	25.1 ± 3.0	14.6 ± 2.4*	1.72 ± 0.08
J_{PDH}	2.02 ± 0.52	3.40 ± 1.60	0.59 ± 0.11

Note. The conditions are as for Table II, except that media were supplemented with either [1-¹⁴C]lactate/pyruvate (0.1 μ Ci/ μ mol) or [2-¹⁴C]lactate plus pyruvate (0.4 μ Ci/ μ mol). Results are expressed as means ± SE for five cell preparations for each cell type.

* $P < 0.05$.

Anterograd & Retrograd perfusion (Tissue Scale)

Time dependent changes in glucose, oxygen & pyruvate under retrograde and anterograde perfusion and giving glucagon.

Constantin1994 [10], Constantin1995 [11]

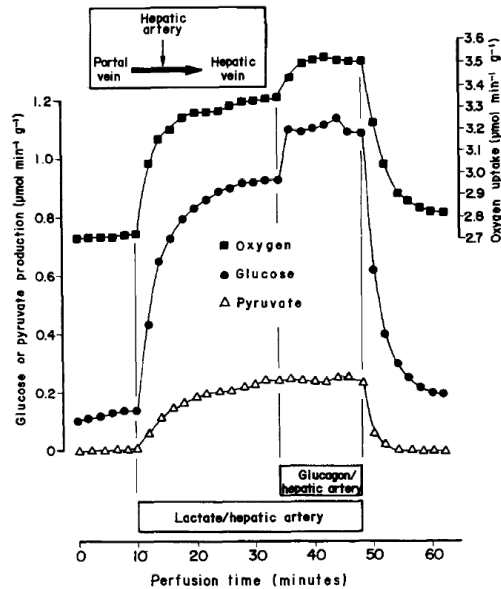


Fig. 1. Effects of glucagon infused into the hepatic artery on gluconeogenesis from lactate infused into the hepatic artery in anterograde perfusion. A liver from a 24-h fasted rat was perfused in the anterograde mode as described in section 2. Lactate ($10 \mu\text{mol} \cdot \text{min}^{-1} \cdot \text{g}^{-1}$) and glucagon ($0.035 \text{ nmol} \cdot \text{min}^{-1} \cdot \text{g}^{-1}$) were infused at the times indicated by the horizontal bars. $[^3\text{H}]\text{Water}$ was infused simultaneously for monitoring the recovery of the fluid pumped into the hepatic artery (not shown). Samples were taken for the measurement of glucose and pyruvate concentration. Oxygen concentration was measured polagraphically.

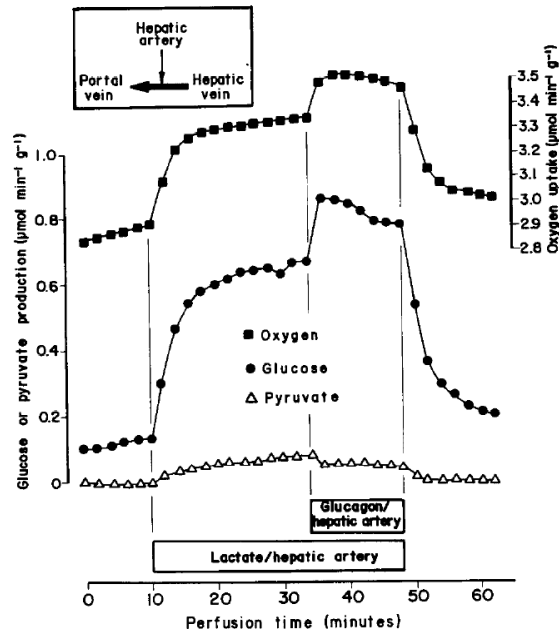


Fig. 2. Effects of glucagon infused into the hepatic artery on gluconeogenesis from lactate infused into the hepatic artery in retrograde perfusion. A liver from a 24-h fasted rat was perfused in the retrograde mode as described in section 2. Lactate ($10 \mu\text{mol} \cdot \text{min}^{-1} \cdot \text{g}^{-1}$) and glucagon ($0.035 \text{ nmol} \cdot \text{min}^{-1} \cdot \text{g}^{-1}$) were infused at the times indicated by the horizontal bars. $[^3\text{H}]\text{Water}$ was infused simultaneously for monitoring the recovery of the fluid pumped into the hepatic artery (not shown). Samples were taken for the measurement of glucose and pyruvate concentration. Oxygen concentration was measured polagraphically.

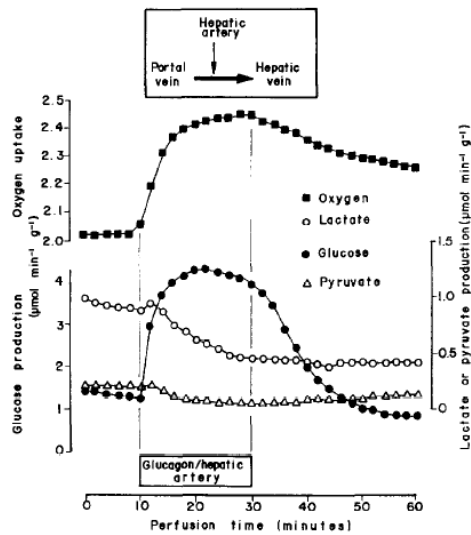


Fig. 2. Effects of glucagon infused into the hepatic artery on oxygen uptake and glycogen catabolism in rat livers perfused bivascularly in the anterograde mode. Livers from fed rats were perfused as described in Section 2. Glucagon was infused into the hepatic artery at a rate of $35 \text{ pmol min}^{-1} \text{ g}^{-1}$ at 10–30 min. Samples of the effluent perfusate were taken for the measurement of glucose, lactate and pyruvate. The venous oxygen concentration was measured polarographically. The data points are the mean of six liver perfusion experiments with identical protocol.

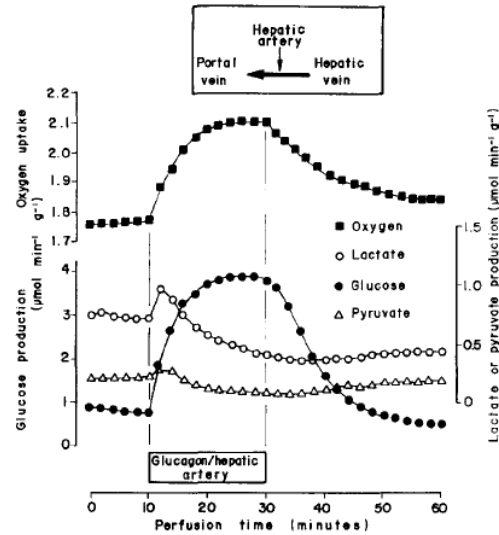


Fig. 3. Effects of glucagon infused into the hepatic artery on oxygen uptake and glycogen catabolism in rat livers perfused bivascularly in the retrograde mode. Livers from fed rats were perfused as described in Section 2. Glucagon was infused into the hepatic artery at a rate of $35 \text{ pmol min}^{-1} \text{ g}^{-1}$ at 10–30 min. Samples of the effluent perfusate were taken for the measurement of glucose, lactate and pyruvate. The venous oxygen concentration was measured polarographically. The data points are the mean of nine liver perfusion experiments with identical protocol.

Effective sinusoidal influent and effluent oxygen partial pressures in isolated rat liver. (Kekonen1987 [12])

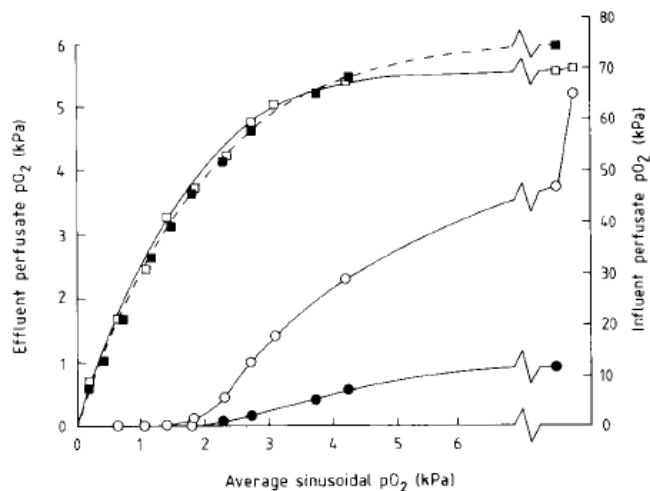


Fig. 1. Correlations between average effective sinusoidal, influent, and effluent oxygen partial pressures in isolated perfused rat liver. A rat liver was perfused with Krebs-Henseleit bicarbonate solution containing 0.1 mM hemoglobin and the influent pO_2 varied by appropriate proportioning of the gas mixtures O_2/CO_2 (19:1) and N_2/CO_2 (19:1). Perfusate flow was $5.1 \text{ ml} \cdot \text{min}^{-1} \cdot \text{g}^{-1} \text{ wet wt.}$ The average effective sinusoidal pO_2 was determined by measuring Hb oxygenation grade optically by transmittance spectrophotometry of a liver lobe simultaneously at 578, 585, and 605 nm as described in Materials and Methods. Symbols: (○—○) Effluent in forward perfusion, (●—●) effluent in reverse perfusion; (□—□) influent in forward perfusion; (■—■) influent in reverse perfusion.

Oxygen consumption/uptake & glucose production under lactate titration (Matsumura1984 [3])

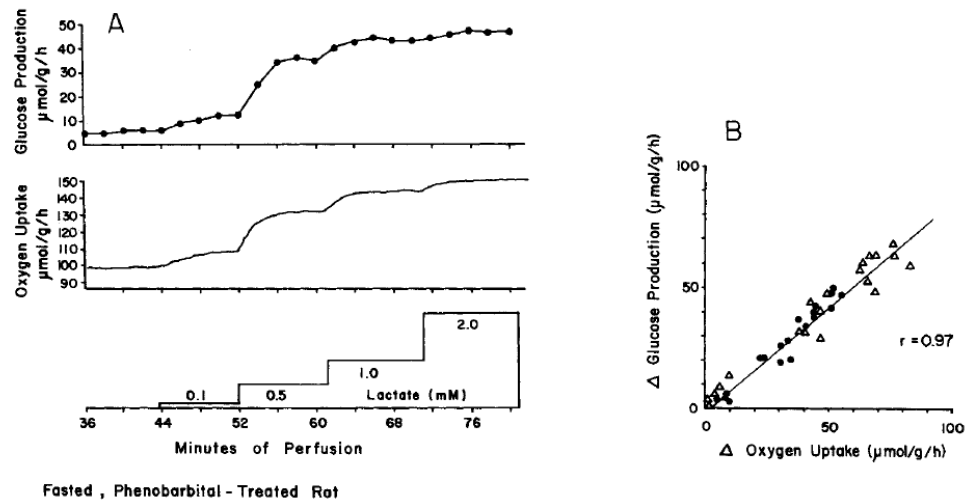


Fig. 1. Titration of gluconeogenesis and O_2 uptake in perfused liver with lactate (A) and correlation between rates of glucose production and extra oxygen uptake in whole liver following the addition of lactate (B). (A) Phenobarbital-treated rats were starved for 24 h before experiments. Livers were perfused with Krebs-Henseleit bicarbonate buffer (pH 7.4, 37°C) in a nonrecirculating system in the anterograde direction. Lactate was infused in the concentrations indicated by the horizontal bar using a precision infusion pump. Upper panel: production of glucose. Middle panel: oxygen uptake. Rates were calculated from the arterio-venous concentration differences and constant flow rate. Typical experiment. (B) Best fit linear regression line from data from five livers perfused in the presence (Δ) and five livers perfused in the absence of epinephrine ($0.1 \mu\text{M}$; \bullet) at five different lactate concentrations (0.1–2.0 mM) as in A

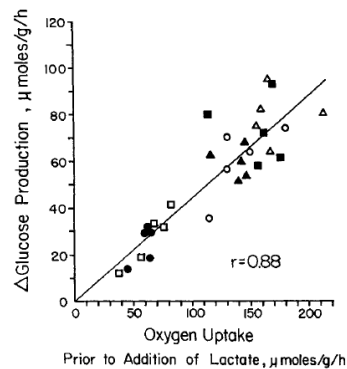


Fig. 5. Relationship between basal oxygen uptake prior to addition of lactate and subsequent rates of gluconeogenesis in periportal and pericentral regions of the liver lobule. Rates of glucose production were determined in periportal (\circ , Δ) and pericentral regions of the liver lobule (\bullet , \blacktriangle) when 2 mM lactate was infused in the presence (Δ , \blacktriangle) or absence (\circ , \bullet) of $0.1 \mu\text{M}$ epinephrine in livers perfused in the anterograde direction. Similar experiments were performed in the retrograde direction in the absence of epinephrine: periportal (\square); pericentral (\blacksquare). Other conditions as in Fig. 3 and Table 3

Effect of glucose on oxygen concentrations and lactate&pyruvate production (Matsumura1984a [13])

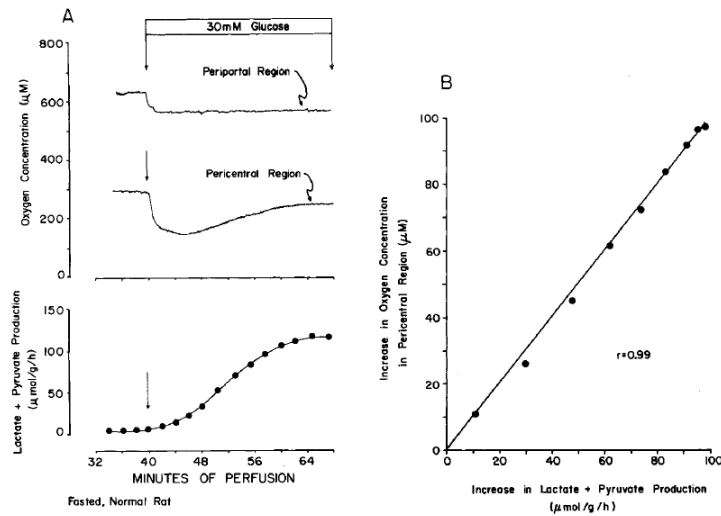


Fig. 2. Effect of glucose on oxygen concentrations in periportal and pericentral regions and lactate + pyruvate production of a liver perfused in the anterograde direction. Rats were starved for 24 h prior to experiments. Miniature oxygen electrodes were placed on periportal and pericentral regions of the liver surface to monitor oxygen concentration of a liver lobule. Glucose was infused in the anterograde direction as indicated by the arrow (arterial concentration, 30 mM). (A) Upper panel: original recording of oxygen concentration in periportal and pericentral areas. Lower panel: rate of lactate + pyruvate production measured in effluent samples. Typical experiment. (B) Relationship between increase in pericentral oxygen concentration and rate of lactate + pyruvate production. Increase in oxygen concentration in pericentral regions was plotted against the increase in rates of lactate + pyruvate production between 6 and 30 min after infusion of glucose. Data from experiments typified by A

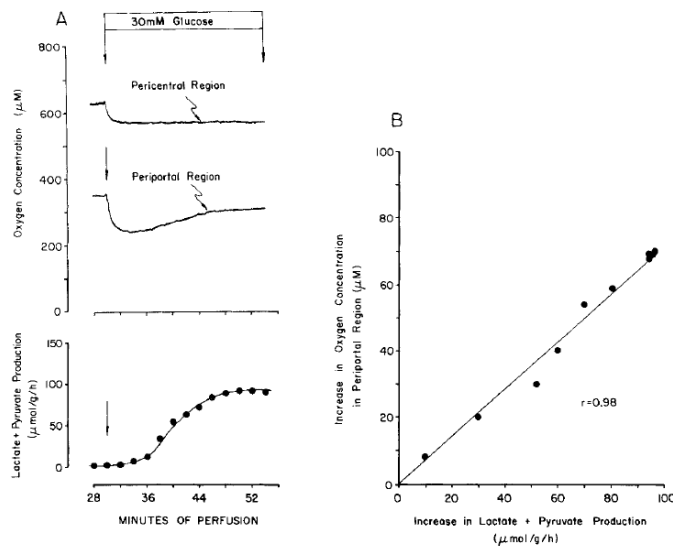


Fig. 3. Effect of glucose on oxygen concentration in periportal and pericentral regions and lactate + pyruvate production in a liver perfused in the retrograde direction. Experimental condition is similar to Fig. 2 except for retrograde perfusion. (A) Upper panel: original recording of oxygen concentration in periportal and pericentral areas. Lower panel: rate of lactate + pyruvate production measured in effluent samples. Typical experiment. (B) Relationship between increase in periportal oxygen concentration and rate of lactate + pyruvate production. Data from experiments typified by Fig. 2A

Heterogeneous glycogen storage (Tissue Scale)

Time dependent glycogen patterns periportal/perivenous.

Babcock1974 [14], Corrin1968 [15]

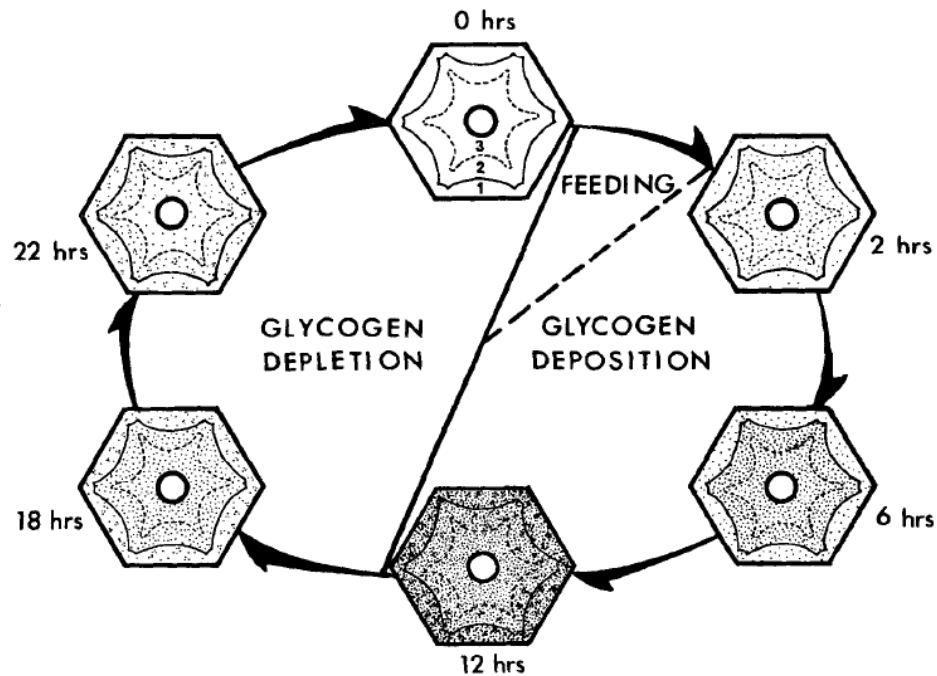


Fig. 3 Summary of hepatic glycogen patterns in rats on a controlled cycle of feeding (2 hours) and fasting (22 hours). Hexagons representing liver lobules with the central veins situated centrally are subdivided into areas designated: (1) periportal, (2) midlobular, and (3) centrilobular.

Signalling (Zonated signalling)

Differences in phosphorylation of metabolic enzymes periportal and perivenous due to glucagon.

Aggarwal1995 [16], Cortinovis1993 [17]

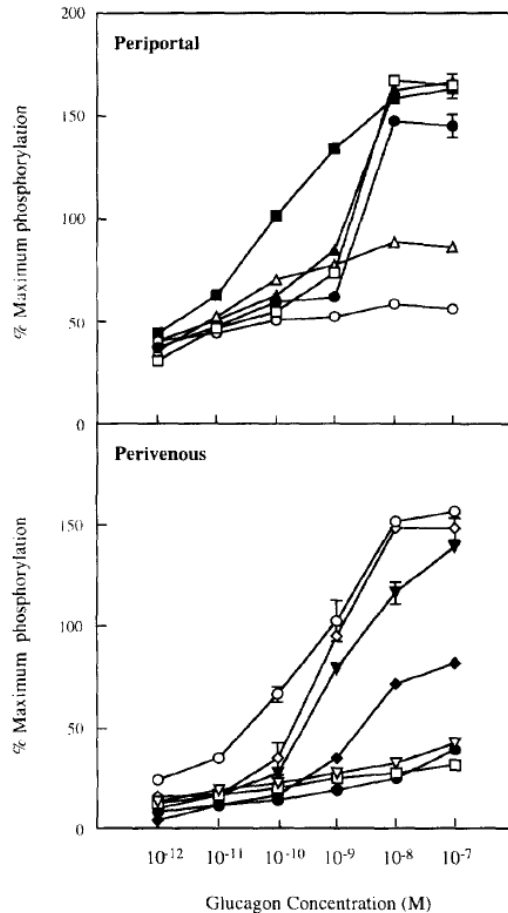


Fig. 2. The phosphorylation of cytosolic peptides in response to different concentrations of glucagon (10^{-12} – 10^{-7} M) in isolated periportal and perivenous hepatocytes. The results shown are means \pm S.E.M. for six separate experiments, the extent of 32 P-labelling of the individual peptides being expressed as increases (%) above basal (no glucagon) values. The phosphopeptides shown are glycogen phosphorylase (\square), glycogen synthase (\bullet), pyruvate kinase (\circ), phenylalanine hydroxylase (Δ), fructose 1,6-bisphosphatase (\blacksquare), the β -subunit of glycogen phosphorylase kinase (∇), fructose 6-phosphate 2-kinase (\blacktriangledown), ribosomal protein S6 (\blacklozenge) and two as yet unidentified peptides of molecular masses of 48 kDa (\blacktriangle) and 46 kDa (\blacklozenge).

TABLE 1. Adenylate cyclase activity in pericentral and periportal microdissected rat liver samples^a

Additions	cAMP produced (pmol \cdot min ⁻¹ \cdot mg dry wt ⁻¹)	
	Pericentral samples	Periportal samples
None (basal)	1.4 \pm 0.1 (41) ^a	1.9 \pm 0.2 (27) ^b
GTP (10 μ mol/L)	2.1 \pm 0.15 (49) ^c	2.8 \pm 0.3 (42) ^{b, c}
Glucagon (1 μ mol/L) + GTP	7.9 \pm 0.7 (35) ^{c, d}	13.1 \pm 2.4 (28) ^{b, c, d}
Isoproterenol (10 μ mol/L) + GTP	2.4 \pm 0.05 (11) ^c	3.6 \pm 0.1 (11) ^{b, c, d}
LiCl (50 μ mol/L)	3.3 \pm 0.9 (10) ^c	4.1 \pm 0.9 (10) ^{b, c}
Angiotensin II (1 μ mol/L) + LiCl	3.1 \pm 0.7 (9) ^c	4.1 \pm 1.0 (10) ^{b, c}
Cholera toxin (50 μ g/ml) + GTP	18.6 \pm 3.0 (24) ^{c, d}	27.7 \pm 3.8 (19) ^{b, c, d}
Pertussis toxin (20 μ g/ml) + GTP	2.2 \pm 0.3 (25) ^c	2.8 \pm 0.5 (20) ^{b, c}
GTP- γ S (10 μ mol/L)	18.9 \pm 1.1 (25) ^c	28.2 \pm 3.1 (20) ^{b, c}
NaF (20 mmol/L)	12.2 \pm 2.6 (25) ^c	18.0 \pm 4.3 (23) ^{b, c}
Forskolin (100 μ mol/L)	27.8 \pm 2.4 (66) ^c	37.9 \pm 4.5 (46) ^{b, c}

^aData expressed as mean \pm S.E.M. from four rats. The number of determinations is given in parenthesis.

^bSignificant compared with corresponding values in pericentral samples by an F-test for paired data: $p < 0.05$.

^cSignificant compared with basal activity by an F-test for paired data: $p < 0.05$.

^dSignificant compared with GTP-stimulated activity by an F-test for paired data: $p < 0.05$.

Glucagon binding periportal and perivenous and changes in cAMP levels. (Ikezawa1998 [8])

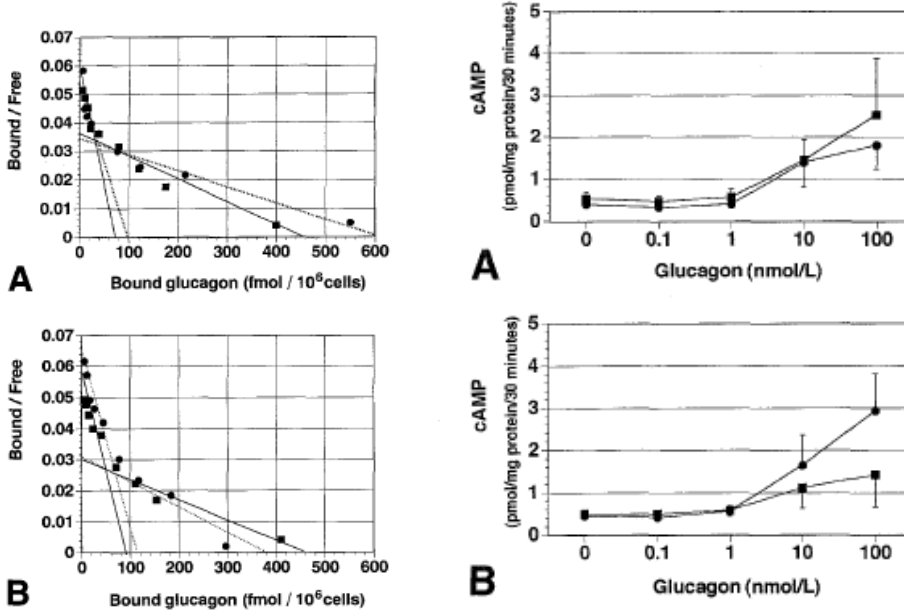


Fig 2. The Scatchard's plot that calculated from the specific binding of [¹²⁵I]-labeled glucagon to PPHs (■) and PVHs (●) of fed normal Wistar rats (A) and of 24-hour fasted normal Wistar rats (B). Values are means of triplicates.

Fig 3. The effect of glucagon on cAMP output from PPHs (■) and PVHs (●) of fed (A) or 24-hour fasted (B) normal Wistar rats. A, PPH (n = 5), PVH (n = 5). B, PPH (n = 5), PVH (n = 4). Detectable level, 0.3 pmol/mg protein/30 minutes.

Insulin binding periportal and perivenous (Ikezawa2001 [18])

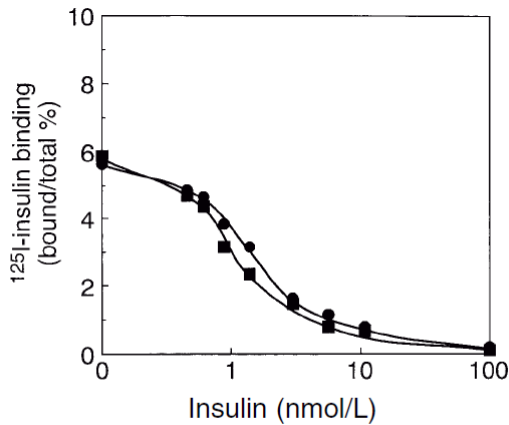


Fig 4. Binding of iodine 125-labeled insulin to PPHs (circles) and PVHs (squares) from fed rats. Each point shows the mean of triplicates.

Zonal distribution of cAMP PDE activity from fed and fasted rats (Runge1991 [19])

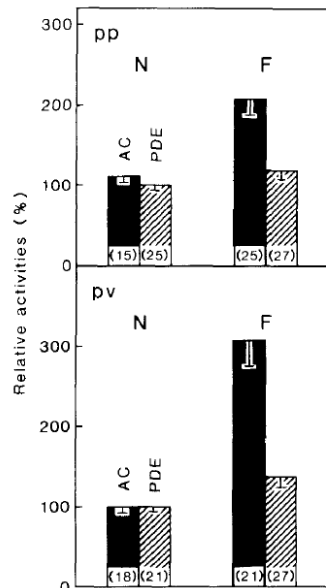


Fig. 3. Capacities for the synthesis and degradation of cyclic AMP in microdissected periportal and perivenous liver tissue of fed and fasted rats. The perivenous activities of glucagon-activated adenylate cyclase (AC) and cGMP-stimulated cyclic AMP phosphodiesterase (PDE) in the fed state were set equal to 100%. Values are means \pm SEM. The number of determinations from 3–4 animals is given in parentheses. The data of glucagon activated AC are taken from Zierz and Jungermann (1984); the data of cyclic GMP-stimulated PDE are from Table 3; *pp* = periportal, *pv* = perivenous; *N* = normal fed; *F* = 48 h fasted

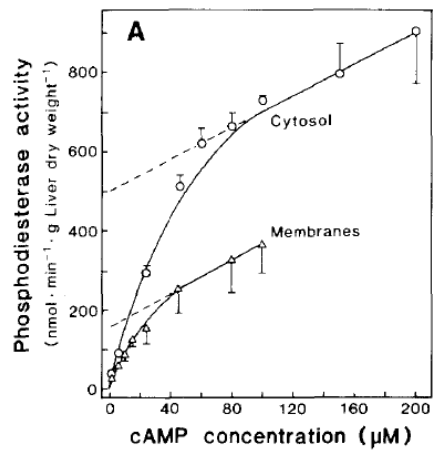


Table 2. Zonal distribution of cyclic AMP phosphodiesterase activity at saturating cyclic AMP concentrations in livers from fed and fasted rats. The enzyme activity was determined with $46 \mu\text{M}$ [^3H]cAMP as described under “Materials and methods”. Mean

values \pm SD of three animals in each dietary state. The number of determinations is given in parentheses. The periportal vs. perivenous values were compared by Student’s *t*-test; n.s. = not significant

State	Enzyme activity [nmol \times min $^{-1}$ \times g dry weight]				
	Homogenate	Periportal (pp)	Perivenous (pv)	pp/pv	p
Fed	823 \pm 99 (3)	847 \pm 140 (28)	937 \pm 167 (24)	0.90	<0.05
Fasted 24 h	685 \pm 116 (3)	639 \pm 183 (28)	734 \pm 220 (25)	0.87	n.s.
Fasted 48 h	581 \pm 31 (3)	539 \pm 123 (24)	709 \pm 134 (25)	0.76	<0.001

Glucagon dependent adenylate cyclase activity (Zierz1984 [20])

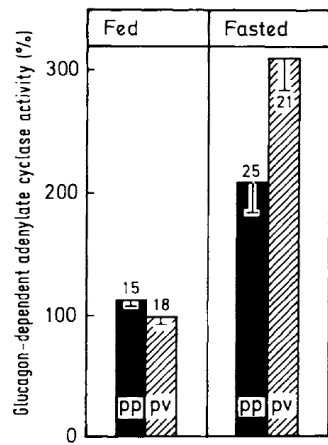


Fig. 3. Distribution pattern of the glucagon-dependent adenylate cyclase in periportal and perivenous liver tissue of fed and fasted rats. The perivenous activity in responsive samples in the fed state was set equal to 100%. Columns represent means \pm SEM (cf. Table 3). The number of determinations is given on top of the columns, the periportal (pp) and perivenous (pv) values were compared by Student's *t*-test; $P < 0.01$ for the activities in fasted rats

Dynamic Zonation & mRNA/protein adaptations

Shortterm O₂ modulation (Woelfle1983[21])

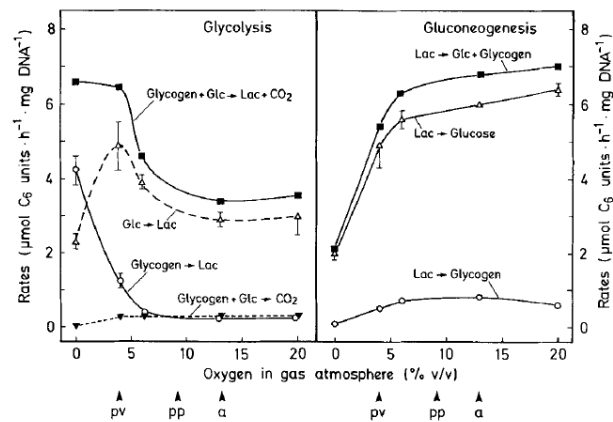


Fig. 2. Glycolysis and gluconeogenesis in cultured hepatocytes under different oxygen tensions. Glycolysis was measured in 'perivenous' cells, gluconeogenesis in 'periportal' cells. The appropriate data are taken from Table 1. Abbreviations as in Fig. 1

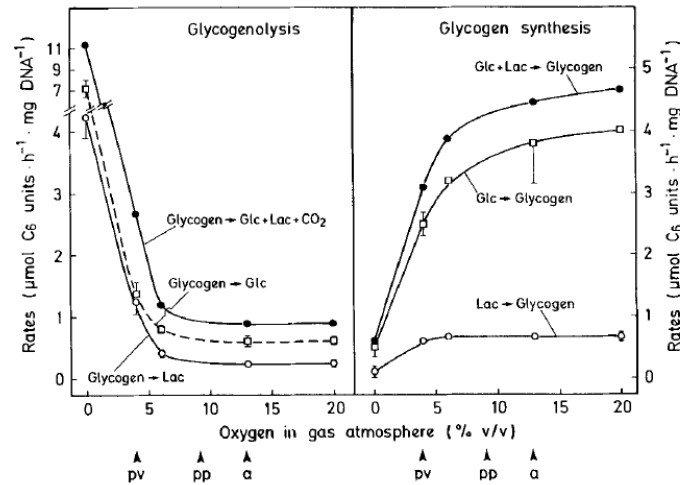


Fig. 1. Glycogenolysis and glycogen synthesis in cultured hepatocytes under different oxygen tensions. Metabolic rates were measured in 'perivenous' cells. The appropriate data were taken from Table 1. Glc = glucose; Lac = lactate. The 'perivenous' (pv) oxygen tension is approximately mimicked by 4% O₂, the 'periportal' (pp) by 9% O₂ and the arterial (a) by 13% O₂

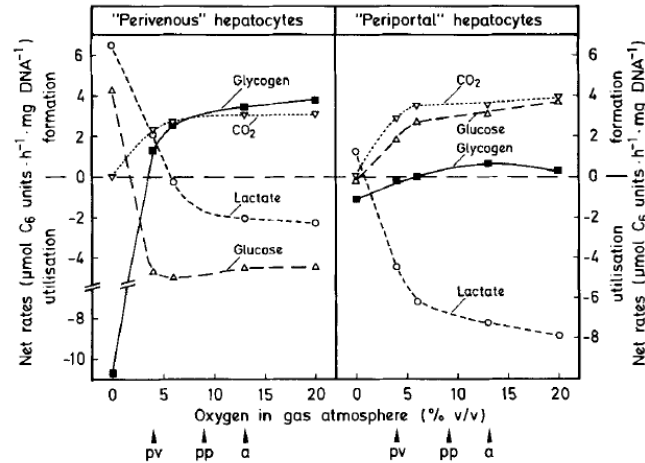


Fig. 3. Glycogen, glucose and lactate metabolism (net rates) in cultured hepatocytes under different oxygen tensions. Net glycogen metabolism is the difference between glycogen breakdown to glucose, lactate and CO₂ and glycogen synthesis from glucose and lactate (Table 1). Net glucose metabolism is the difference between glucose conversion to glycogen, lactate and CO₂ and glucose formation from glycogen and lactate (Table 1). Net lactate metabolism is the difference between lactate conversion to glycogen, glucose and CO₂ and lactate formation from glycogen and glucose (Table 1). Abbreviations as in Fig. 1

Long-term O₂ modulation (Woelfle1985 [22])

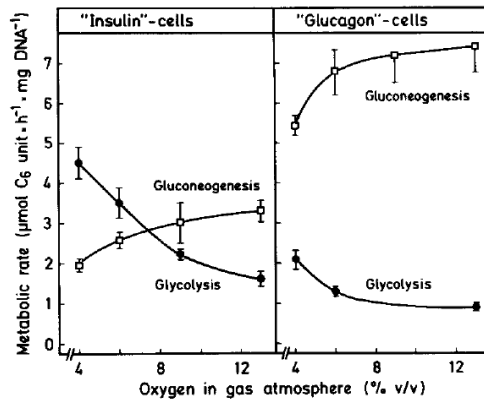


Fig. 1. Overall long-term effects of different oxygen tensions on metabolic rates in hepatocytes. Cells were cultured for 46 h with insulin or glucagon as the major hormone (10 nM) and dexamethasone (10 nM) under the indicated oxygen atmospheres with gentle shaking (20 rev./min). Metabolic rates were measured for 2 h after the last medium change with 5 mM glucose and 2 mM lactate under the same indicated oxygen concentrations. Either glucose or lactate were ¹⁴C-labeled. Values are means \pm SEM of eight cultures from at least three different cell preparations

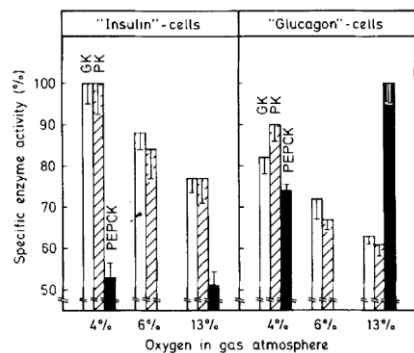


Fig. 2. Enzyme activities in hepatocytes cultured under different oxygen tensions. Cells were cultured for 46 h under the hormonal conditions and oxygen tensions as in Fig. 1. Enzyme activities were assayed 2 h after the last medium change. Values are means \pm SEM of at least six cultures from two different cell preparations; they are given on a percentage basis. The 100% values for glucokinase (GK) and pyruvate kinase (PK) were those measured in insulin cells at 4% O_2 , whereas the 100% value for phosphoenolpyruvate carboxykinase (PEPCK) was that measured in glucagon cells at 13%; the values in $\mu\text{mol} \times \text{min}^{-1} \times \text{mg DNA}^{-1}$ were: GK 0.3; PK 20 and PEPCK 0.4

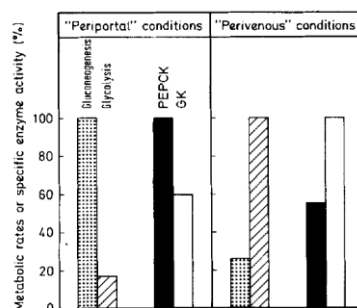
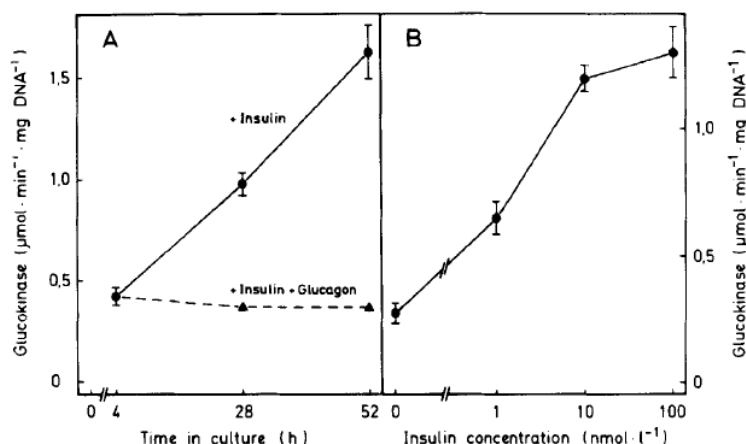


Fig. 3. Comparison of the metabolic rates and enzyme equipment of hepatocytes cultured and tested under 'periportal' and 'perivenous' conditions. As discussed in the text 13% O_2 and a predominance of glucagon (10 nM) should best mimic periportal conditions, 4% O_2 and a prevalence of insulin (10 nM) perivenous conditions. The metabolic rates are taken from Fig. 1, the enzyme activities from Fig. 2. The 100% values are: gluconeogenesis and phosphoenolpyruvate carboxykinase (PEPCK) in glucagon cells under 13% O_2 , $7.3 \mu\text{mol} \times \text{h}^{-1} \times \text{mg DNA}^{-1}$ and $0.4 \mu\text{mol} \times \text{min}^{-1} \times \text{mg DNA}^{-1}$, respectively; glycolysis and glucokinase (GK) in insulin cells under 4% O_2 , $4.6 \mu\text{mol} \times \text{h}^{-1} \times \text{mg DNA}^{-1}$ and $0.3 \mu\text{mol} \times \text{min}^{-1} \times \text{mg DNA}^{-1}$, respectively

GK induction glucagon (Jungermann1982 [4])

FIG. 2. Induction of glucokinase in primary cultures of rat hepatocytes by insulin in the presence of dexamethasone (74). Liver parenchymal cells were cultured under standard conditions (Fig. 1). Four and 28 hr after plating the medium was changed. In (A), insulin (10^{-7} moles per liter) with or without glucagon (2×10^{-7} moles per liter), and in (B), insulin, at the concentrations indicated, was added with each medium change. Enzyme activity was measured in (A) at the time points indicated and in (B) at 52 hr. Values are mean \pm S.E. of six cultures from two representative experiments.



mRNA modulation of GK and PCK by oxygen (Kietzmann1997 [23])

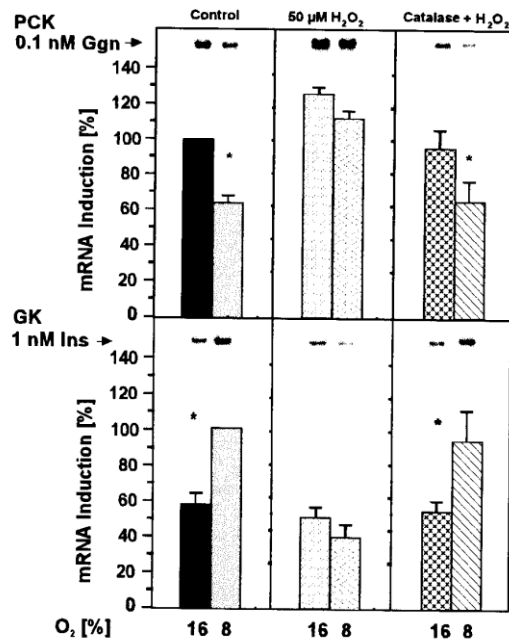


Figure 6. Modulation by oxygen of the glucagon-dependent activation of the phosphoenolpyruvate carboxykinase (PCK) gene and of the insulin-dependent activation of the glucokinase (GK) gene in cultured rat hepatocytes. Simulation of arterial P_{O_2} by H_2O_2 . Hepatocytes were cultured for 24 h under standard conditions with an atmosphere of 16% (v/v) oxygen. Then the PCK gene was activated by the addition of fresh medium containing 0.1 nmol/L glucagon; the GK gene was activated by adding 1 nmol/L insulin to the cultures without a medium change. Both hormone concentrations are half-maximally effective physiological concentrations. The culture was then continued at 16% O_2 or 8% O_2 , mimicking periportal and perivenous O_2 tensions, respectively. With the oxygen tensions applied, the decrease due to diffusion of oxygen through the medium to the cell surface was taken into consideration. The cells were harvested after 2 h (PCK) or 3 h (GK) of induction, i.e., when the mRNA levels of PCK or GK, respectively, were maximal. The mRNA levels were quantified by videodensitometry of northern blots of total RNA. The maximal increase in mRNA was set equal to 100% in each single experiment. Values are means \pm SEM from 4 independent cultures. For details see Kietzmann et al. (1996, 1997b).

PEPCK induction by oxygen, insulin & glucagon (Jungermann1986 [24])

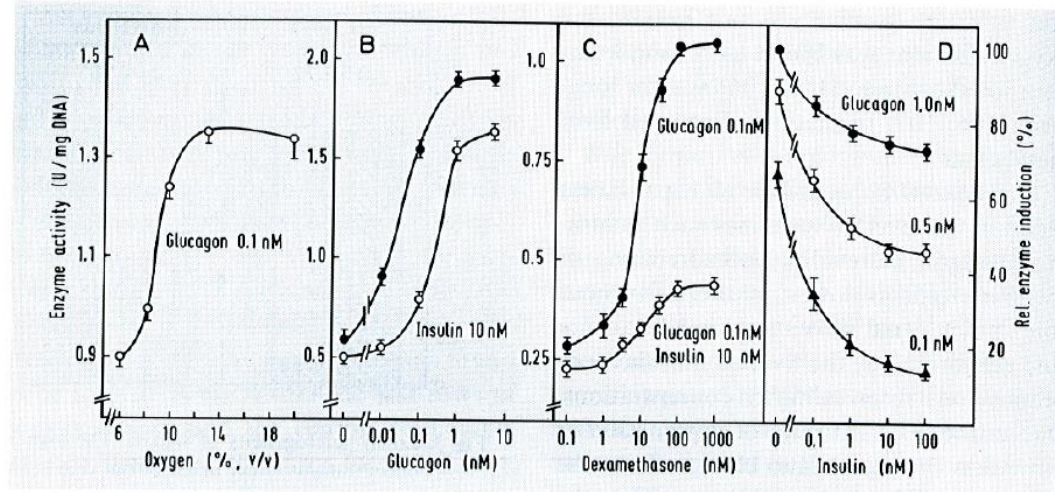


Fig. 4. Induction of phosphoenolpyruvate carboxykinase by glucagon. Modulation by oxygen, antagonism by insulin and permissive action of dexamethasone. Cells were cultured for 24 h with 1 nmol/l (panel A) or 0.5 nmol/l insulin and either with 0.1 μmol/l dexamethasone (panel B and D) or with different dexamethasone concentrations as shown (panel C). The gas atmosphere contained 13% (v/v) oxygen (panels B–D) or the percentage shown (panel A). Gluca-

gon \pm insulin in the indicated concentrations were added at 24 h and enzyme activity was measured at 28 h. In panel A the uninduced activity corresponded to 0.35 U/mg DNA; in panel D relative enzyme induction from 0 to 100% corresponds to the uninduced and the fully induced enzyme activity, i.e. 0.6–1.9 U/mg DNA. Values are means \pm SEM of nine dishes from three different cell preparations for each panel. For details see references 107 and 112.

Changes in GK and HK rat liver after start of glucose feeding. (Toyoda1995 [25])

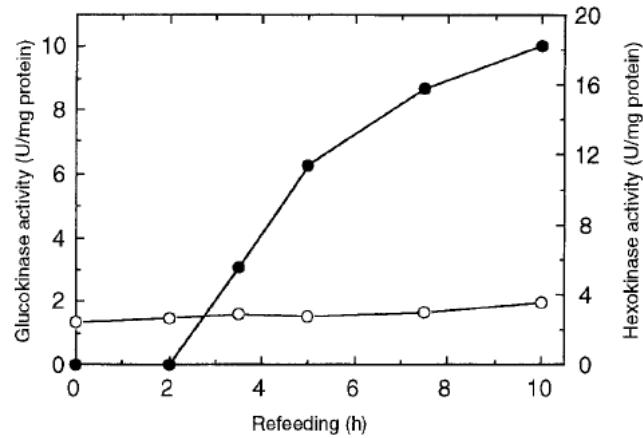


Fig. 2 Changes in glucokinase and hexokinase activities in rat liver after the start of glucose refeeding. ●, Glucokinase activity; ○, hexokinase activity

Effects of starvation and refeeding on the intra-acinar distribution pattern of PEPCK (Wimmer1989 [26], Wimmer1990 [27])

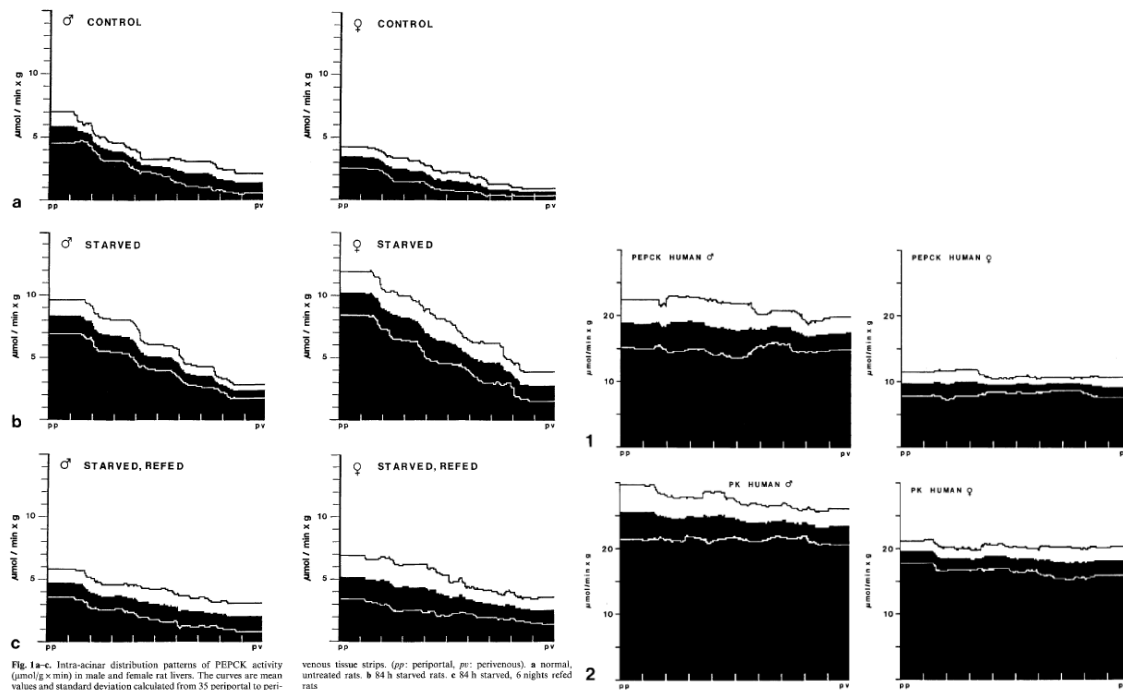


Fig. 1a-c. Intra-acinar distribution patterns of PEPCK activity ($\mu\text{mol/g} \times \text{min}$) in male and female rat livers. The curves are mean values and standard deviation calculated from 35 periportal to per-

venous tissue strips. (pp: periportal, pv: perivenous). **a** normal, unstarved rats. **b** 84 h starved rats. **c** 84 h starved, 6 nights re-fed rats

mRNA gradients along sinusoid (PEPCK) starved and fed mouse liver (Ruijter2004 [28])

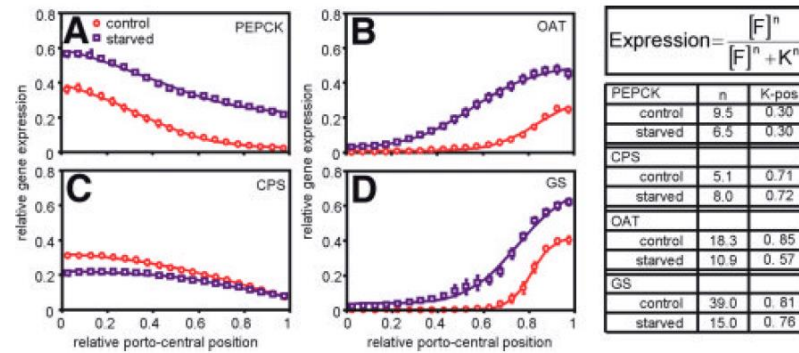
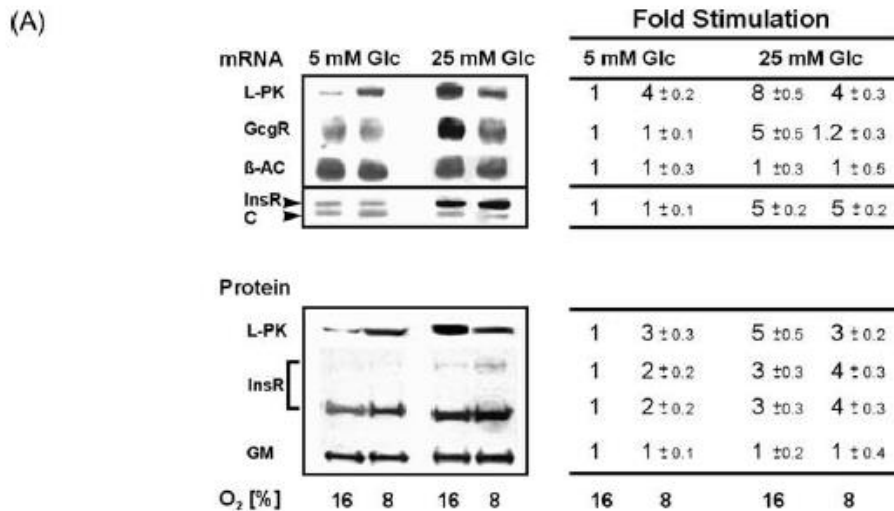


Fig. 9. Gene expression gradients in control and starved mice. The gene expression gradients were measured (cf. Fig. 3) for the periportally expressed enzymes (A) PEPCK and (C) CPS, and for the pericentrally expressed enzymes (B) OAT and (D) GS. The OD values per zone are linearly related to the mRNA concentration¹⁷ and can be used as a direct estimate of the relative level of gene expression. The affinity and cooperativity parameters that resulted when the gradients were fitted to a model for hepatic gene expression² are given in the table. The affinity constant (K) was made independent of the assumed signal-factor gradient by converting it to K-pos, the position on the porto-central axis where the expression gradient reaches its point of inflection.

mRNA modulation by glucose and oxygen (HIF interplay) (Kietzmann2002 [29])



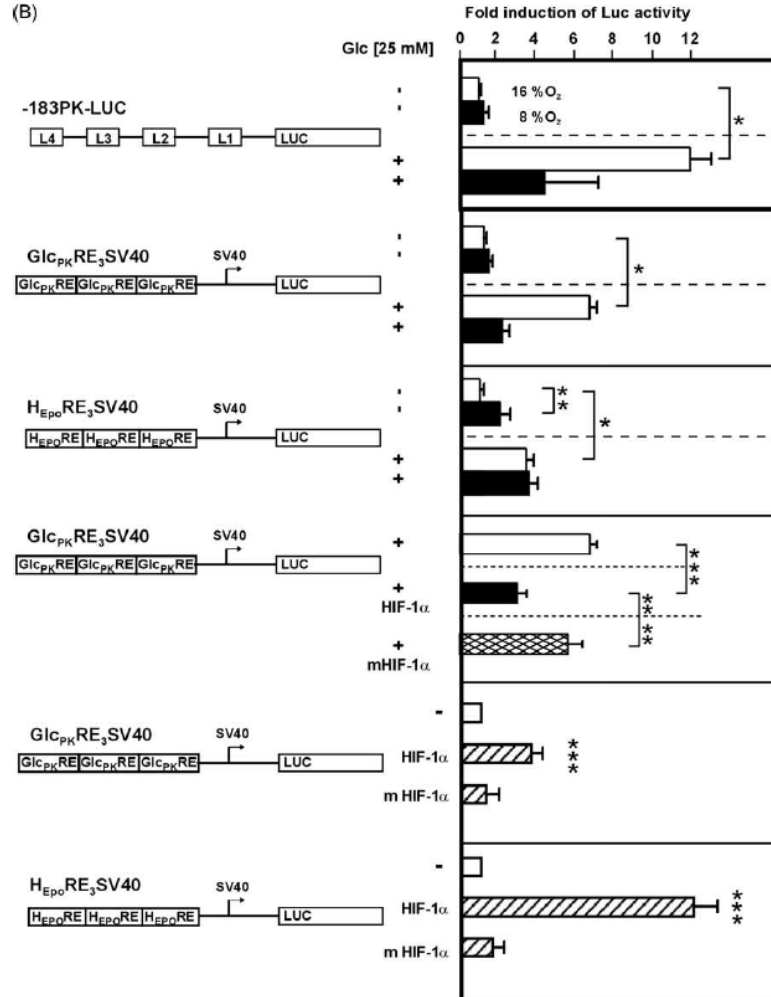


Fig. 2. Induction of L-PK expression by perivenous pO₂ and by glucose under periportal but not perivenous pO₂ in primary rat hepatocyte cultures. Modulation by hypoxia-inducible factor 1. (A) Primary rat hepatocytes were cultured for 24 hr under arterial pO₂ (16% O₂) at basal glucose levels (5 mM) of the culture medium M199. Then glucose was added to the final indicated concentrations and the cells were further cultured under arterial and venous pO₂ (8% O₂) for another 24 hr. Northern blots with RNA from cultured rat hepatocytes were hybridized to a DIG-labeled L-PK, GcgR or β -actin (β -AC) antisense RNA probe. Insulin receptor (InsR) mRNA levels were estimated by quantitative RT-PCR analysis (for details, see [12,13,50]). For Western analysis cells were cultured as described above. Total protein was analyzed by blotting using an antibody against L-PK, InsR or as control with an antibody against Golgi membrane (GM), cf. [50]. Values are means \pm SEM of three independent culture experiments. L-PK was visible as a band of 60 kDa, the InsR β -chain was visible as two bands of 95 and 69 kDa, GM was visible as a band of 94 kDa. C: competitor; L-PK: L-type pyruvate kinase; GM: Golgi membrane;

Enzyme and metabolic activities over time (Probst1982 [2])

Table 1. *Enzyme and metabolic activities in primary cultures of hepatocytes*
Cells were cultured as described in Fig. 1 for 4 h, 24 h and 48 h. The rates of glycolysis and gluconeogenesis were determined in the presence of 0.5 nM insulin and 0.1 μ M dexamethasone as described by incubating the cells for another 2 h in media containing both glucose (5 mM) and lactate (2 mM) which were reciprocally labelled. Enzyme activities were assayed before and after the 2 h incubation, no difference was observed. Values are means \pm SEM of 12 culture dishes from 4 different cell preparations

Time in culture	Enzyme activity		Metabolic rate	
	glucokinase	p-pyruvate carboxy-kinase	glycolysis	gluconeogenesis
h	$\mu\text{mol} \cdot \text{min}^{-1} \cdot \text{mg DNA}^{-1}$		$\mu\text{mol C}_6 \text{ unit} \cdot \text{h}^{-1} \cdot \text{mg DNA}^{-1}$	
4	0.73 ± 0.05	1.0 ± 0.05	3.2 ± 0.40	6.3 ± 0.45
24	0.65 ± 0.06	0.4 ± 0.03	0.65 ± 0.15	3.2 ± 0.40
48	0.41 ± 0.05	0.21 ± 0.02	1.2 ± 0.10	2.3 ± 0.22

G6Pase Vmax/Km dependency (VanNoorden1995 [30])

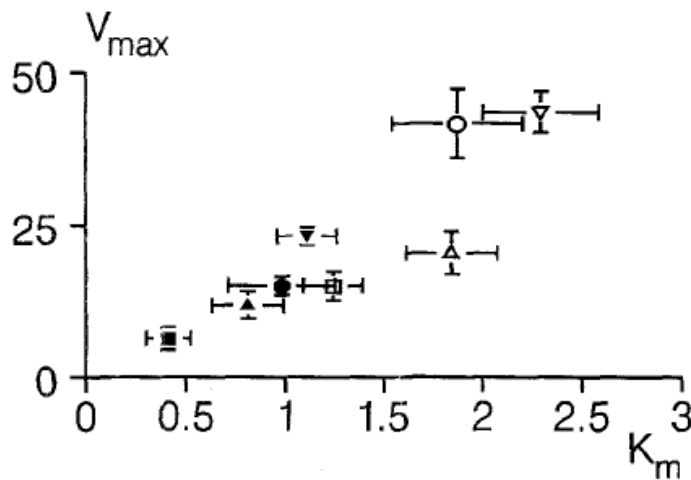
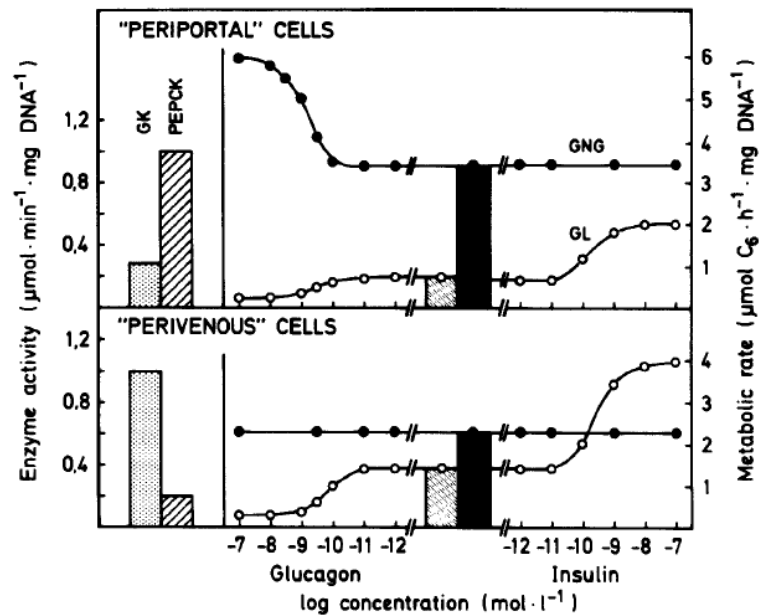


Fig. 6 Relationship between K_m and V_{max} values of glucose-6-phosphatase for glucose-6-phosphate as analysed cytophotometrically in the different zones of rat liver lobules. The mean values \pm standard error of the mean are given for pericentral (■) and periportal (□) zones of fed female rats, for pericentral (▲) and periportal (△) zones of fed male rats, for pericentral (●) and periportal (○) zones of starved female rats and for pericentral (▼) and periportal (▽) zones of starved male rats

Induction of periportal and perivenous hepatocytes via insulin and glucagon (Jungermann1982 [4])

FIG. 4. Induction of "periportal" and "perivenous" hepatocytes in primary cultures of rat hepatocytes. Cells were cultured under standard conditions (Fig. 1). Four hours after plating, the medium was changed: "perivenous" cells were induced for the following 44 hr with another medium change after 20 hr in the presence of insulin (10^{-8} moles per liter) and dexamethasone (10^{-7} moles per liter); "periportal" cells were induced in the presence of glucagon (10^{-8} moles per liter), dexamethasone (10^{-7} moles per liter), and insulin (5×10^{-10} moles per liter). Metabolic rates were determined radiochemically (83) by incubating the washed cells for another 2 hr in media containing both glucose (5 mmoles per liter) and lactate (2 mmoles per liter), which were reciprocally labeled and hormones as indicated. Glycolysis (GL) was quantitated by measuring [^{14}C]lactate formation from [^{14}C]glucose and gluconeogenesis (GNG) by determining [^{14}C]glucose production from [^{14}C]lactate. Enzyme activities (GK, glucokinase; PEPCK, phosphoenolpyruvate carboxykinase) were assayed both before and after the incubation for the study of metabolic rates; no difference was observed. Values are means of three cultures from a representative experiment (I. Probst and K. Jungermann, preliminary results).



- [1] Peak, M., Agius, L., Differential incorporation of gluconeogenic precursors and glucose into glycogen in periportal and perivenous rat hepatocytes. *Biochem Soc Trans* 1990, 18, 587-588.
- [2] Probst, I., Schwartz, P., Jungermann, K., Induction in primary culture of 'gluconeogenic' and 'glycolytic' hepatocytes resembling periportal and perivenous cells. *European journal of biochemistry / FEBS* 1982, 126, 271-278.
- [3] Matsumura, T., Kashiwagi, T., Meren, H., Thurman, R. G., Gluconeogenesis predominates in periportal regions of the liver lobule. *European journal of biochemistry / FEBS* 1984, 144, 409-415.
- [4] Jungermann, K., Katz, N., Functional hepatocellular heterogeneity. *Hepatology* 1982, 2, 385-395.
- [5] Jungermann, K., Heilbronn, R., Katz, N., Sasse, D., The glucose/glucose-6-phosphate cycle in the periportal and perivenous zone of rat liver. *European journal of biochemistry / FEBS* 1982, 123, 429-436.
- [6] Shiota, M., Inagami, M., Fujimoto, Y., Moriyama, M., *et al.*, Cold acclimation induces zonal heterogeneity in gluconeogenic responses to glucagon in rat liver lobule. *The American journal of physiology* 1995, 268, E1184-E1191.
- [7] Tosh, D., Alberti, G. M., Agius, L., Glucagon regulation of gluconeogenesis and ketogenesis in periportal and perivenous rat hepatocytes. Heterogeneity of hormone action and of the mitochondrial redox state. *Biochem J* 1988, 256, 197-204.
- [8] Ikezawa, Y., Yamatani, K., Ogawa, A., Ohnuma, H., *et al.*, Effects of glucagon on glycogenolysis and gluconeogenesis are region-specific in periportal and perivenous hepatocytes. *J Lab Clin Med* 1998, 132, 547-555.
- [9] Jones, C. G., Titheradge, M. A., Measurement of metabolic fluxes through pyruvate kinase, phosphoenolpyruvate carboxykinase, pyruvate dehydrogenase, and pyruvate carboxylate in hepatocytes of different acinar origin. *Arch Biochem Biophys* 1996, 326, 202-206.
- [10] Constantin, J., Ishii-Iwamoto, E., Suzuki-Kemmelmeier, F., Bracht, A., Zonation of the action of glucagon on gluconeogenesis studied in the bivascularly perfused rat liver. *FEBS letters* 1994, 352, 24-26.
- [11] Constantin, J., Ishii-Iwamoto, E. L., Suzuki-Kemmelmeier, F., Yamamoto, N. S., Bracht, A., The action of glucagon infused via the hepatic artery in anterograde and retrograde perfusion of the rat liver is not a function of the accessible cellular spaces. *Biochim Biophys Acta* 1995, 1244, 169-178.
- [12] Kekonen, E. M., Jauhonen, V. P., Hassinen, I. E., Oxygen and substrate dependence of hepatic cellular respiration: sinusoidal oxygen gradient and effects of ethanol in isolated perfused liver and hepatocytes. *Journal of cellular physiology* 1987, 133, 119-126.
- [13] Matsumura, T., Thurman, R. G., Predominance of glycolysis in pericentral regions of the liver lobule. *European journal of biochemistry / FEBS* 1984, 140, 229-234.
- [14] Babcock, M. B., Cardell, J., RR, Hepatic glycogen patterns in fasted and fed rats. *Am J Anat* 1974, 140, 299-337.
- [15] Corrin, B., Aterman, K., The pattern of glycogen distribution in the liver. *Am J Anat* 1968, 122, 57-72.
- [16] Aggarwal, S. R., Lindros, K. O., Palmer, T. N., Glucagon stimulates phosphorylation of different peptides in isolated periportal and perivenous hepatocytes. *FEBS letters* 1995, 377, 439-443.
- [17] Cortinovis, C., Klimek, F., Nogueira, E., Adenylate cyclase activity in microdissected rat liver tissue: periportal to pericentral activity gradient. *Hepatology* 1993, 18, 160-164.
- [18] Ikezawa, Y., Yamatani, K., Ohnuma, H., Igarashi, M., *et al.*, Insulin inhibits glucagon-induced glycogenolysis in perivenous hepatocytes specifically. *J Lab Clin Med* 2001, 138, 387-392.
- [19] Runge, D., Jungermann, K., Distribution of cyclic AMP phosphodiesterase in microdissected periportal and perivenous rat liver tissue with different dietary states. *Histochemistry* 1991, 96, 87-92.
- [20] Zierz, S., Jungermann, K., Alteration with dietary state of the activity and zonal distribution of adenylate cyclase stimulated by glucagon, fluoride and forskolin in microdissected rat liver tissue. *European journal of biochemistry / FEBS* 1984, 145, 499-504.
- [21] Wölflle, D., Schmidt, H., Jungermann, K., Short-term modulation of glycogen metabolism, glycolysis and gluconeogenesis by physiological oxygen concentrations in hepatocyte cultures. *European journal of biochemistry / FEBS* 1983, 135, 405-412.
- [22] Wölflle, D., Jungermann, K., Long-term effects of physiological oxygen concentrations on glycolysis and gluconeogenesis in hepatocyte cultures. *European journal of biochemistry / FEBS* 1985, 151, 299-303.
- [23] Kietzmann, T., Jungermann, K., Modulation by oxygen of zonal gene expression in liver studied in primary rat hepatocyte cultures. *Cell Biol Toxicol* 1997, 13, 243-255.

- [24] Jungermann, K., Functional heterogeneity of periportal and perivenous hepatocytes. *Enzyme* 1986, *35*, 161-180.
- [25] Toyoda, Y., Miwa, I., Kamiya, M., Ogiso, S., *et al.*, Tissue and subcellular distribution of glucokinase in rat liver and their changes during fasting-refeeding. *Histochem Cell Biol* 1995, *103*, 31-38.
- [26] Wimmer, M., Effects of starvation and refeeding a high carbohydrate diet on the intra-acinar distribution pattern of phosphoenolpyruvate carboxykinase activity in the liver of male and female rats. *Histochemistry* 1989, *92*, 331-336.
- [27] Wimmer, M., Luttringer, C., Colombi, M., Enzyme activity patterns of phosphoenolpyruvate carboxykinase, pyruvate kinase, glucose-6-phosphate-dehydrogenase and malic enzyme in human liver. *Histochemistry* 1990, *93*, 409-415.
- [28] Ruijter, J. M., Gieling, R. G., Markman, M. M., Hagoort, J., Lamers, W. H., Stereological measurement of porto-central gradients in gene expression in mouse liver. *Hepatology* 2004, *39*, 343-352.
- [29] Kietzmann, T., Krones-Herzig, A., Jungermann, K., Signaling cross-talk between hypoxia and glucose via hypoxia-inducible factor 1 and glucose response elements. *Biochem Pharmacol* 2002, *64*, 903-911.
- [30] Van Noorden, C. J., Jonges, G. N., Heterogeneity of kinetic parameters of enzymes in situ in rat liver lobules. *Histochem Cell Biol* 1995, *103*, 93-101.